Journal of Network Intelligence
Taiwan Ubiquitous Information
 ISSN 2414-8105 (Online)
Volume **6**, Number **4**, November **2021**

Neural network based model for image detection in seismic electromagnetic wave

Wei Ding
Key Laboratory of Earthquake Geodesy, CEA
Institute of Seismology, CEA
Hubei Earthquake Administration
Wuhan, China
tingwhere@163.com

Ji Han*
Jackie Chan movie and media college
Wuhan Institute of Design and Sciences
Wuhan,China
Corresponding author: kingham850707@163.com

Lan Song
Electrical and Computer Engineering
Faculty of Engineering and Applied Science
Memorial University
St. Johns, NL, Canada, A1B 3X5
sl130com@163.com

Dijin Wang
Key Laboratory of Earthquake Geodesy, CEA
Institute of Seismology, CEA
Hubei Earthquake Administration
Wuhan, China
wangdijin@126.com

Received June 2021; revised August 2021

Abstract. *The composition of natural seismic electromagnet signals recorded by seismic instruments is complex, which cannot be directly used to analyze ground motion events information with common text data analysis methods. The fractal dimension of seismic trace time series are used to study the similarity of seismic waves in the characteristics of complex geological structures and breakpoint locations. The basis of extracting seismic electromagnet waveform image texture feature is to realize image recognition. Two-dimensional waveform texture features can be used to identify two-dimensional time-amplitude seismic waveform signals. This paper proposes the application of STFT algorithm to curve fitting of seismic electromagnetic waveform signal, which can be used to generate the filled and binarized seismic waveform image. An improved VGG neural network is used to realize the identification of related images, which transform electromagnetic signal recognition into an object detection problem. 1437 real-time earthquake cases collected from 165 stations in Sichuan-Yunnan region are applied to verify the performance of VGG model. The result shows that the training and detection accuracy rate of the data set can reach 90%. The seismic electromagnetic signals processed by the STFT algorithm are more conducive to seismic identification, and suitable image features can be extracted, which has certain reference value for the identification of small sets of natural seismic events.*
Keywords: seismic electromagnetic, short time Fourier transform, deep learning, target detection, convolutional neural network

1. **Introduction.** The natural seismic wave signal components recorded by seismic observation instruments are complicated. A single analysis method and its parameters cannot reflect the essential characteristics of the seismic event. A large number of observations and studies have shown that electromagnetic anomalies will be generated before moderate and strong earthquakes. This electromagnetic anomaly is not only observed on the ground, but also on satellites [1]. Therefore, seismic electromagnetic signals can be used as an important reference basis for seismic events. The existence of abnormal ionospheric disturbances before large earthquakes in space, such as TEC (total electron content of electric ions), has been statistically verified. However, the observation of electromagnetic anomalies on the ground is often interfered by a variety of factors, and there is an urgent need for new observation instruments and observation methods to find correlation. Acoustic and electromagnetic testing all in one system (AETA) [2], a system of observing electromagnetic anomalies on the surface, has high-sensitivity probes and high-precision data acquisition systems, and can be used as an improved observation of electromagnetic anomalies on the surface through large-scale deployment.

In the field of seismic waveform identification, different from the previous time and frequency domain analysis methods [3, 4], image recognition has become a more popular method for studying the characteristics of seismic events [5]. Using the form of early visualization, the obscure and irregular seismic waveform data can be turned into an intuitive and clear graphical form. This work proposes an improved short-time Fourier transform (STFT) preprocessing, i.e., FFT (fast Fourier transform) is performed on a series of windowed electromagnetic data, and each of the frame frequency-domain signal by Fourier transform is stacked in time domain to obtain spectrogram. An improved VGG16 architecture neural network is used to identify the seismic electromagnetic STFT-based image signals. The distinguishing experimental consisting of 1437 real-time earthquake cases collected from 215 stations shows that the training and detection accuracy rate of the image data set can reach 90%, which can meet the requirements of identifying seismic electromagnet signal images.

This paper is an enhance version of our previous seismic electromagnet signal work published in proceedings of the CIS 2020 conference. The remainder of this paper is organized as follows. In Section 2, we describe the related works for identifying weak signals, seismic machine learning methods, and application of analyzing seismic electromagnetic signals. The design principle and research method for identifying seismic electromagnet signals and improved VGG16 model are presented in Section 3. Section 4 implement of the model for identifying seismic electromaget signals . Section 5 presents the results and discussions of using STFT in data collection phase for improved VGG model. The conclusions and future research directions for STFT-based seismic electromagnet signal identification are outlined in Section 6.

2. **Related work.** As a method of data mining for identifying weak signals, principal component analysis (PCA) is utilized to analyze seismic electromagnetic signals and separate signals from noise [6, 7]. For example, the solar radiation period 27 day was used as sliding time window to detect quartile difference threshold [8]. Local correlation tracking method is more suitable for non-stationary signal processing compared with classical cross-correlation method. This method is based on the good spatial correlation between the magnetic field components of different ELF stations to pick up the correlation coefficient to achieve the purpose of weak anomalies signals identification. As a case study of the M4.6 Jinggu earthquake in Yunnan, China, the LCT method to the magnetic-filed

data processing as well, and the results of both north-south and east-west magnetic field components showed that local correlation coefficient saw anomalies about a week before the earthquake [9]. The wavelet transform method is used to process the earth resistivity observation data of seismic electromagnetic signals of the Chengdu and Jiangyou station before and after the 2008 Wenchuan M_s8.0 earthquake, the Wenchuan earthquake, and the DEMETER satellite records before and after the 2010 Haiti M_w7.0 earthquake. The ionospheric magnetic field observation data are used to analyze the wavelet energy spectrum of earth resistivity and ionospheric magnetic field and their relative changes [10]. Numerical simulation algorithms have been applied to the time-domain and frequency-domain characteristics of the seismic waves and the accompanying electromagnetic signals generated under the action of dual-couple point sources and finite fault plane sources in different structural models. The result shows that the type of seismic source time functions affect the seismic wave field value simulation results [11].

Various machine learning methods have been applied to sismology. For example, Lin et al. introduces convolutional neural network deep learning methods for intelligent extraction, classification and identification of seismic oil and gas features [12]. On the basis of the automatic recognition of the arrival time of P wave by the Ren AIC algorithm, Ren et al applid the Bagging machine learning algorithm to distinguish the nature of the seismic event [13]. Han et.al employ machine learning as an abnormal data mining model for reducing error of mean square. The vector value and the seismic monitoring data extracted from raw data were calculated in a library for data feature [14]. Li and Cai used adversarial networks in machine learning to distinguish the first P wave arrival time and applied the result in earthquake early warning [15, 16]. Chen employed unsupervised learning to identify microseismic events, which introduced fuzzy clustering algorithm to improve the method [17]. To the best of our knowledge, the above works are correlated with discrimination of seismic wave arrival time and seismic phase identification. However, there is lack of research on distinguishing seismic electromagnetics using convolutional neural network [18, 19].

3. **Design Principles of electromagnetic image recogenization.**

3.1. **Data collected from AETA.**

The devices of AETA system are composed of electromagnetic high precision sensing probes, data acquisition unit, and data analysis unit for each device [20]. As shown in Figure 1., the seismic electromagnetic observation station is represented by blue dots, and the recorded seismic data is represented by red dots. Seismic electromagnetic observation stations are mainly distributed in the Sichuan-Yunnan region of China where earthquakes occur frequently. The distribution of stations is convenient for recording real seismic data.

A device of AETA system consists of various sensors, e.g., a pressure sensor, an earth sound probe, and seismic electromagnetic detecting probe. In this work, we use seismic electromagnetic probe to obtain the amplitude of the seismic electromagnetic signal with additional latitude and longitude information. The selection criteria of magnitude is earthquake above Mw3.6 and the epicenter distance needs to be less than 75KM, e.g., earthquake in Yushu (96.7E, 33.10N) recorded by station Yushu (97.01E, 32.08N). In the end, we selected 1,437 paired earthquake events as the data set for the subsequent machine learning process. The earthquake data set collected by the same instrument 14 days before the earthquake and 14 days after the earthquake are used as comparative samples. Unrecorded and full range data are dropped out using manual screening. To avoid interference, the two types of data sets are randomly arranged out of order.

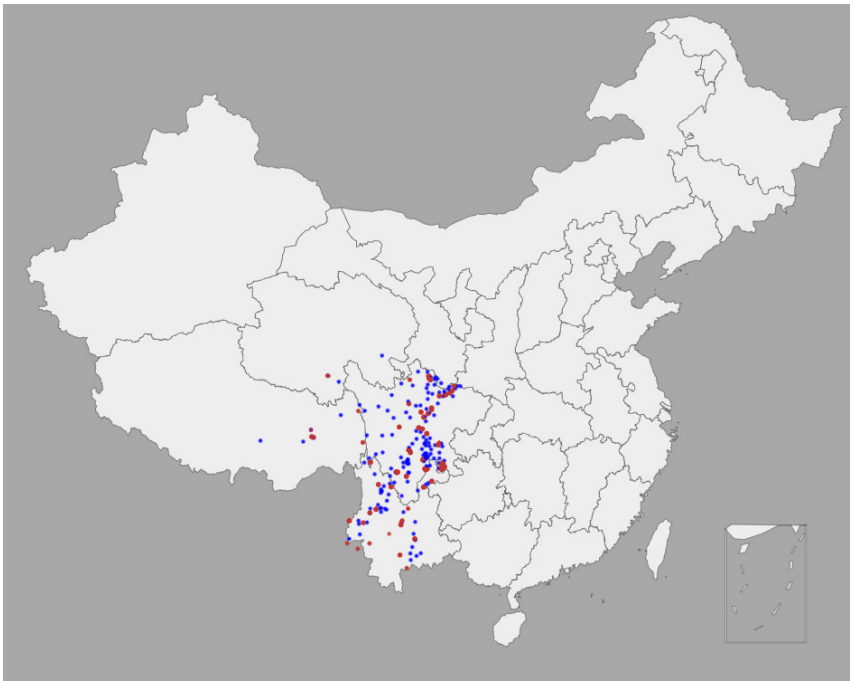

FIGURE 1. Seismic electromagnetic observation station and selected earthquake distribution

3.2. **Improved DTFT for seismic electromagnetic.** Short-time Fourier transform (STFT) is widely used simple and intuitive method for studying non-stationary signals [21] . Given a signal $x(t) \in L2(R)$, its STFT is defined as (1) and (2)

$$STFT_x(t,\Omega) = \int x(\tau) g_{t,\Omega}(\tau) d\tau = \int x(\tau) g^*(\tau - t) e^{j\Omega\tau} d\tau \tag{1}$$

$$\frac{1}{2\pi}\int_{-\infty}^{\infty} X(v) G^*(v-G) e^{j(v-\Omega)t} d\Omega = e^{-j\Omega t}\frac{1}{2\pi}\int_{-\infty}^{\infty} X(v) G^*(v-G) e^{jvt} d\Omega \tag{2}$$

where $\|g(\tau)\| = 1$, $\| g_{t,\Omega}(\tau) \| = 1$ and the window function $g(\tau)$ should be a symmetric function . Its basic idea is to use the window function $g(\tau)$ to cut $x(\tau)$ in the time domain, i.e., change the time variables of $x(t)$, $g(t)$ to τ, and perform the Fourier transform of the truncated local signal. The Fourier transform of the signal at a certain moment can be obtained. When the center position of the window function $g(\tau)$ keeps changing position, the Fourier transforms at different moments are available for analyzing. The set of these Fourier transforms is $STFTx(t,\Omega)$ [22].

In the classic STFT, the non-oscillating low-pass window function is used, which is based on the premise that the signal is stable in a short time interval, but this premise does not exist when the time-varying characteristics of the signal are more significant. Therefore, a high-resolution representation cannot be obtained. In this case, it is more reasonable to approximate the signal within the time interval as a chirp signal. Therefore, the traditional window function is improved, and the following chirp window function is used to substitute the low-pass window function:

$$\gamma(t) = g(t) e^{j\frac{c_t}{2}t^2} \tag{3}$$

$g(t)$ is a low-pass window function, and ct is the chirp index, which is a time function. From the point of view of the instantaneous frequency of the signal, the traditional STFT

depend on a low-pass non-oscillating window function which uses a straight line parallel to the time axis (frequency constant) to approximate the instantaneous frequency curve of the signal, which can be regarded as the instantaneous frequency of the signal. Zero-order approximation, while the STFT using a chirp window function with a variable frequency modulation index uses a diagonal line, i.e., linear change in frequency, to approximate the instantaneous frequency curve of the signal, which can be regarded as a first-order approximation to the signal. In the case of selecting the frequency modulation coefficient appropriately, the STFT using the improved chirp window function can obtain a more accumulated signal time-frequency representation than the traditional STFT. Using improve STFT, the precision of acoustic spectrum for the seismic electromagnetic signal can be improved. A window frame is used to create a specific section, in which can be used to calculate the discrete Fourier transform (DFT) of it. The window moves parallel R point to frame the next section and calculate its DFT. By calculating section to section, which is equivalent to record time nodes manually, the obtained data contains both time and frequency information.

4. **Method for identifying seismic electromagnet signals.**

4.1. **Image recognition using Keras.** As a framework for deep learning architecture, Keras has the advantages of understandability and scalability. The backend of Keras supports multiple network architectures, e.g., Tensorflow, theano, mxnet, and cntk, which can be adopted with custom layer easily. Tensor library of Keras has a highly optimized back-end engine, which can provide advanced building blocks and optimized operations. Keras itself is an intermediate layer. Using Keras to call Tensorflow or theano will be slower than using Tensorflow or theano alone, but it is actually acceptable in small sample target detection, e.g., seismic electromagnetic data set in this work.

4.2. **Converted electromagnetic signal images using libraso.** Librosa module in Python is used to process low-frequency electromagnetic signals, which can be developed for time-frequency processing, feature extraction and converting various signals into images. When selecting window function ω_1 and frame shift R, it needs to satisfy Constant Overlap-Add (COLA):

$$\sum_{-\infty}^{\infty} \omega_1(n - mR) = 1 \tag{4}$$

By setting a suitable value of Constant Overlap Add (COLA), the original signal can be restored by the IDFT result of each frame of the superimposed spectrum, and a waveform graph and its time-frequency diagram can be generated. The COLA requirement is important for avoiding artifacts. The signal is divided into blocks by setting a rectangular window without overlap in librosa. When the rectangular windows overlap by 50%, the shape changes, but the sum of the overlapping parts in the middle is still equal to a constant. The commonly used overlap rate (L-frame shift)/L Hamming window in STFT conforms to COLA, e.g., 1/2, 3/4. For the spectrum analysis used for measuring, the Bartlett window processed for the endpoints and windows in the generalized Hamming family handled correctly are all equal to COLA(M/2) (50% overlap).. The equal weight of COLA ensures that the input data were weighted for each point, which can be completely reconstructed and avoid aliasing. The recording frequency of seismic electromagnetic data is once for a minute. By using librosa module and setting a reasonable COLA value to handle low-frequency signals, which combined by 1440 points a day, the waveform graph

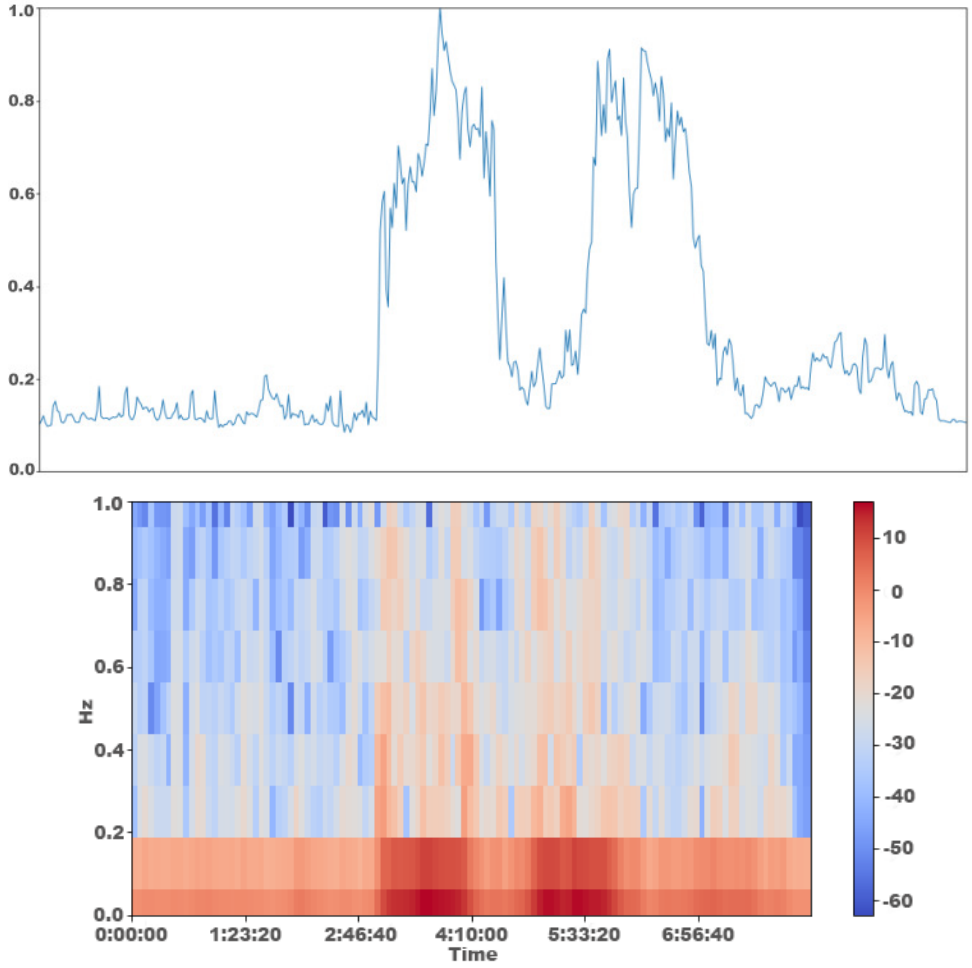

FIGURE 2. A raw electromagnetic signal and its converted STSF form

and its time-frequency diagram can be figured out. Figure 2 shows a sample electromagnetic signal and its STSF form generated from libraso. Note that, Superposition should be distinguished between splicing in librosa. The result of IDFT cannot reveal the seismic electromagnetic signal of each frame directly, i.e., combining these results cannot get a complete seismic electromagnetic signal for a day. The reasons are elaborated as follow: 1. the result of IDFT is not the seismic electromagnetic signal of each frame, but the signal using rectangular window. The result of windowing and framing is predefined before the type of signals is identified and restored, which also leads to overlapping parts between adjacent frames; 2. Due to overlap, Overlap-Add perform superposition rather than splicing [23]. Superimposition can ensure that key seismic information for seismic signal is not lost.

4.3. **Algorithm.** Figure 3. is the schematic diagram of entire algorithm for identifying seismic electromagnetic. The algorithm includes two phases as follows: data conversion and machine learning. The data conversion phase is performed in sequence according to the following steps:1, Preprocessing raw data from AETA, i.e., magnitude and epicentral distance are parsed from raw csv data using regular expressions; 2, normalized, i.e., the range of electromagnetic values is unified to (0,1), which can increase the speed of gradient descent and improve the convergence of the model; 3, Introduce an improved STFT to convert a two-dimensional linear image into a spectrogram image; 4, Vectorization, i.e., converting spectrogram images obtained in step3 into tensors, shuffling the images order

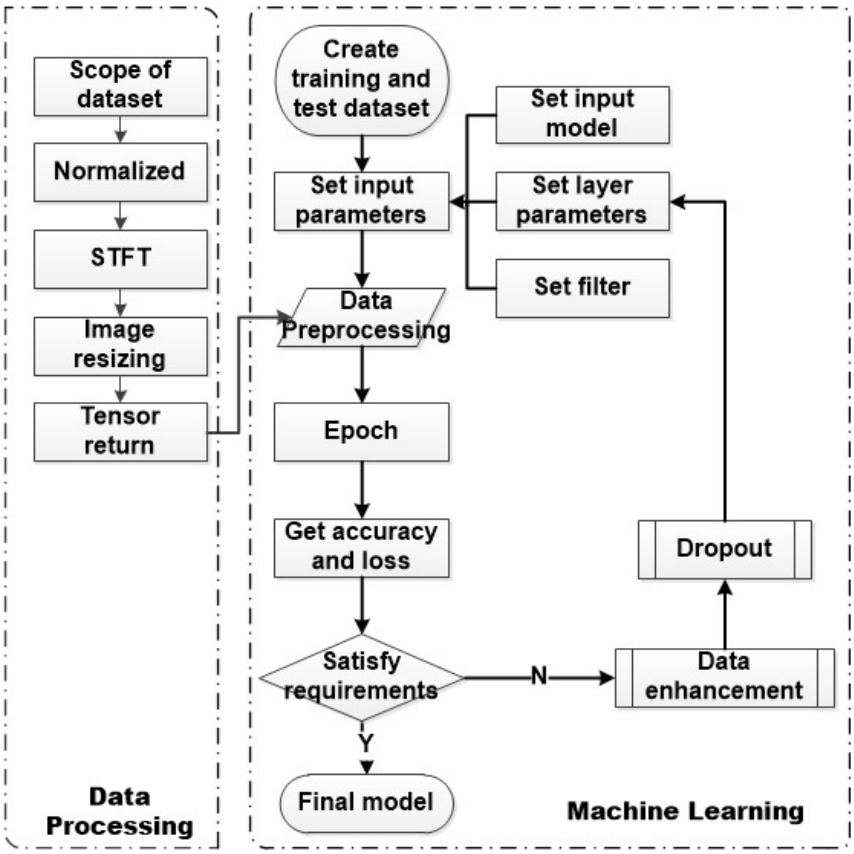

FIGURE 3. Flow chart of distingulishing seismic electromagnetic data

to enhance data, Since seismic electromagnetic signals have a strict time sequence, the traditional flipping and random rotation methods are not suitable for data enhancement in the data preprocessing stage The machine learning phases for seismic electromagnetic will be elaborated in next section. The entire data is divided into two data sets, 14 days before and after the earthquake separately.

4.4. **Improved VGG model.** The images used in this work are spectral waterfall diagrams synthesized after DFT of seismic electromagnetic signals instead of pictures in nature. Based on the VGG16 model, an improved VGG model for seismic electromagnetic signal identification is constructed by modifying several parameters. The architecture of improved model mainly refers to the Inceptionv1 network [24]. Only 3×3 and 1×1 convolution kernels are used to compress the model parameters, and the number of feature channels is doubled after pooling operation, in order to maintain the integrity of the features as much as possible [25, 26]. At the same time, drawing on the idea of Inceptionv2, batch normalization is used for the output of each convolutional layer, which increases the robustness and training speed of the model, and can replace dropout to prevent overfitting. Learn from jump connection idea of ResNet [27], after shaping the output of the previous conv, it is directly combined with the next conv and output to the next layer together, so that the output layer can retain higher-resolution features and reduce the probability of gradient disappearance. Nonlinear activation function ReLU is used to reduce the probability of neuron death during training. The original VGG16 structure and processing process are described as follows.

Input layer: In the seismic time picking problem, the input layer is a 512×512×1 three-dimensional matrix, 1000 represents the number of sampling points in the time domain, 3

represents the three components of N, E, and Z, and 1 represents the depth of the input layer.

Convolutional layer: It builds a receptive field by combining specific convolutional neurons. Each input node in the convolutional layer only selects a small part of the previous layer of neural network, i.e., the convolution kernel, thereby reducing the number of parameters in the final fully connected layer. This paper uses the commonly used convolution kernel size 3×3 in the field of electromagnetic image recognition.

Pooling layer: It can reduce the size of parameter matrix of neural network effectively. The pooling operation reduces the image resolution to facilitate subsequent operations. When convolutional neural networks are applied to classification problems (such as image classification), the pooling layer plays a role in extracting low-frequency summary features. This paper uses a 2×2 pooling layer.

Fully connected layer: After several rounds of convolutional layer processing of electromagnetic images, the image information has been summarized into various features containing higher information.. The convolutional layer can be regarded as a process of automatic image feature extraction. After the feature extraction step is completed, the fully connected layer is utilized to classify the electromagnetic images. Note that, only one fully connected layer is used in this work.

The Rectified linear unit (ReLU) function is applied in activation function layer to calculate the probability that the current sample belongs to different types.

In order to make the model learn fewer errors from the training data, the regulariztion method is used to reduce the overfitting, dropout method is utilized in this model, i.e., randomly discard the modified output features during the training process. Precision is used to measure the loss function. To enhance learning efficiency in model training, the number of layers is modified via distinct architectures. Number of units per layer, L1/L2 regularization, the learning rate, and iterate feature engineering are added to improve efficiency of learning.

Due to the balance of positive and negative ratios in the data set samples, for binary classification tasks, the built-in evaluation index binary_accuracy of keras can be directly used for evaluation. As shown in Figure 4 below, the accuracy rate reaches 90% in the initial stage without the introduction of dropout, which proves that it has been overfitting. In order to eliminate this situation and achieve better model characteristics, the conv_base layer needs to be extended. This effect can be partially eliminated through the improved VGG16 model, which will be elaborated in the next paragraph.

A fine-tuned VGG16 model for different convolutional layers is used to identify the seismic electromagnetic image dataset. The weight parameter of VGG-16 reaches level of 100 million, including 3 fully connected layers to ensure parameter concentration. However, considering that the parameters of VGG16 are designed for 1000 classification categories, this study only needs to use 2 of them which account for a small proportion. The original number of fully connected layers in VGG16 model can be reduced to 2. After several comparative experiments, to improve the recognition accuracy and model efficiency, the first fully connected layer should be 4096, and the second one should be 2. The improved VGG16 model for electromagnetic images still uses a 3×3 convolution kernel, and every two convolutional layers, a maximum pooling layer is used to form the first three groups of convolutional pooling structures. The number of convolution kernels increases according to powers of two, e.g., 32, 64, 128. In order to reduce the computational complexity, the fully connected layer simplifies the complex first three layers of the original VGG16. As shown in Figure 5, the composition details of improved VGG16 are described as follows: When the image input layer is 32×32×3, the first three convolutional networks are all composed of 2 convolutional layers with a convolution kernel size of 3×3 and a maximum

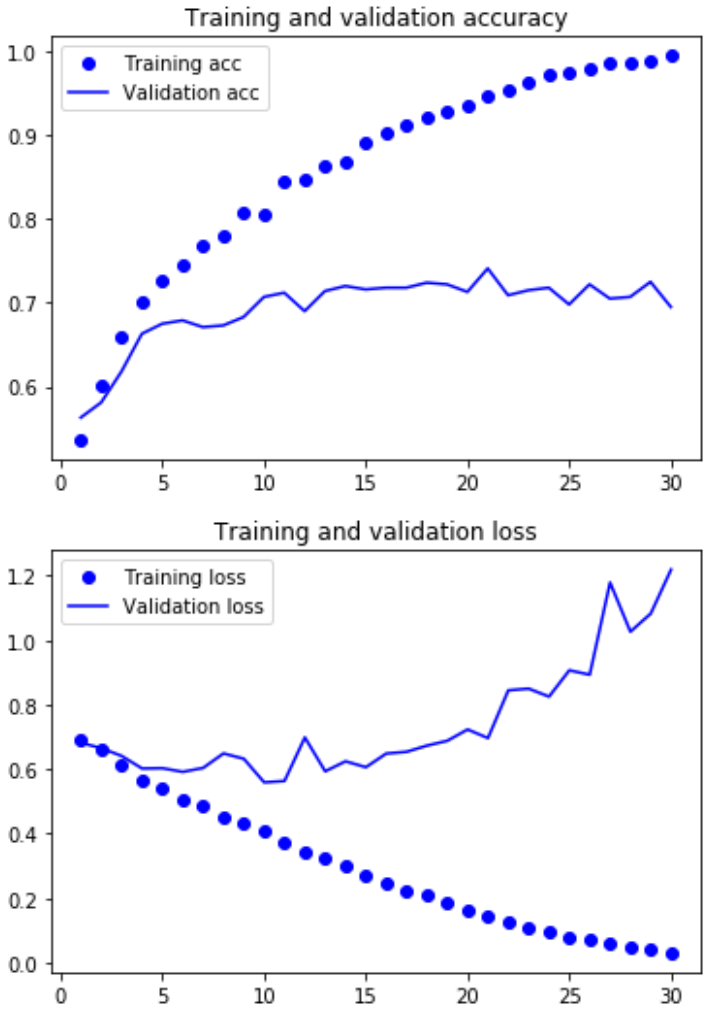

FIGURE 4. The accuracy and loss curves of the training and accuracy sets of 30 epochs using original VGG16 model without dropout

pooling layer. However, in order to keep the number of cores equal, the number of convolution cores is evolved from 32×32×64 to 4×4×256, while the step size is maintained at 1×1.The structure of the following two convolutional networks is similar to the first one. Add the flatten layer to realize the conversion of multi-dimensional input into one-dimensional input, which also can complete the transition from the convolutional layer to the fully connected layer. To reduce over-fitting, the dropout layer is introduced at the end of the improved VGG16 model structure for electromagnetic signals.

5. **Result and discussion.**

5.1. **Result.** By tracking the loss and accuracy rate during the network training process by customizing a callback function, accuracy is used as the target to measure the loss function. As described in former section, The improved VGG16 model enhance learning accuracy by reducing the number of convolution layers using dropout layer, and adding L1/L2 regularization. For example, to expand the original VGG16 architeture, data-enhanced feature extraction can be used to reduce training loss. Note that, the number of sample in dataset is not large enough to completely eliminate the overfitting. When added to a modified filtering layer, gradient descent for input image can be realized to get largest possible filter response, and obtain an image with the maximum filter response.

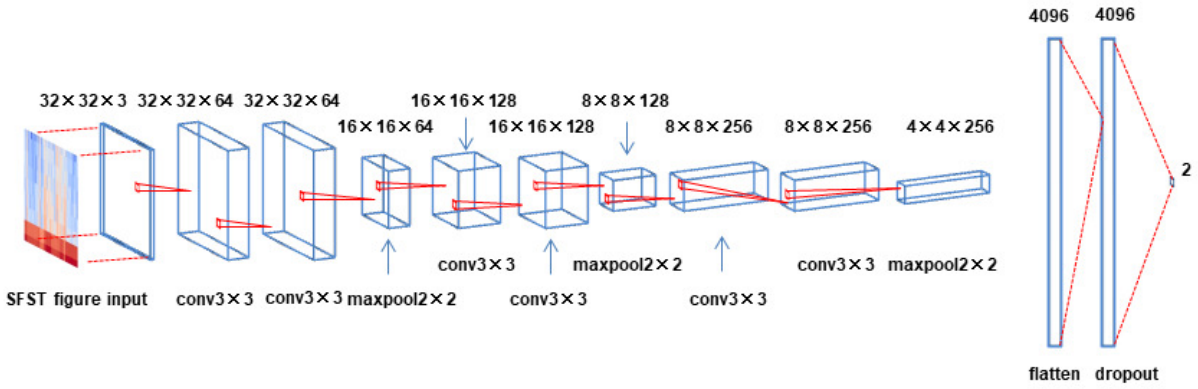

FIGURE 5. An improved VGG model

From Figure 2 , some features of the signal on the spectrogram can be manually identified, which is also the basic premise for using machine learning image classification in this research. Experiments show that the STFT spectrogram generated by the seismic electromagnetic signal can be correctly identified by the improved VGG16 algorithm. Accuracy is the ratio of correctly identified electromagnetic samples to the total number of samples. Accuracy in test dataset can be used to evaluate the performance of the improved VGG16 model. As shown in Figure 6, the accuracy in test set has increased to 90% using refined convolutional networks architecture described in section 4. By observing the decreasing trend of the loss value of the training set and the test set separately, we can get following result: the highest precision setting is using batch size 64. Increasing the batch size will reduce the training time for each training epoch, which will also cause a decrease in accuracy and overfitting. As shown in TABLE I, the different comparison results of various parameters of the improved VGG16 model reflect the improvement of the model performance.

TABLE 1. Comparison results of various batch size of improved VGG16 model

Batch Size	64	128	256	512
Spending Time	90min	60min	56min	54min
Accuracy of the 10th epoch	89.20%	88.12%	87.57%	86.65%
Accuracy of the 100th epoch	94.34%	92.33%	91.42%	91.06%
Loss of the 10th epoch	0.2720	0.2926	0.3070	0.3257
Loss of the 100th epoch	0.1553	0.1942	0.2304	0.2331

5.2. **Discussion. Accuracy of observation instruments data**: In this work, the waveform processing model of the reference did not perform well. One of the reasons is the architecture of the image processing process of librosa is not suitable for general waveform processing, and the parameters are not adjusted to the best state. Further exploration of better architectures and training parameters may improve their performance. In practical applications, the consistency of the electromagnetic observation instruments and the recorded data are greatly affected by the environment. For example, some instruments only record once every 3 minutes, and some instruments are interfered by the surrounding magnetic field, and the valid signals cannot be extracted from noise. To improve the accuracy and resolution of the experiment, instruments with higher signal-to-noise ratio should be deployed.

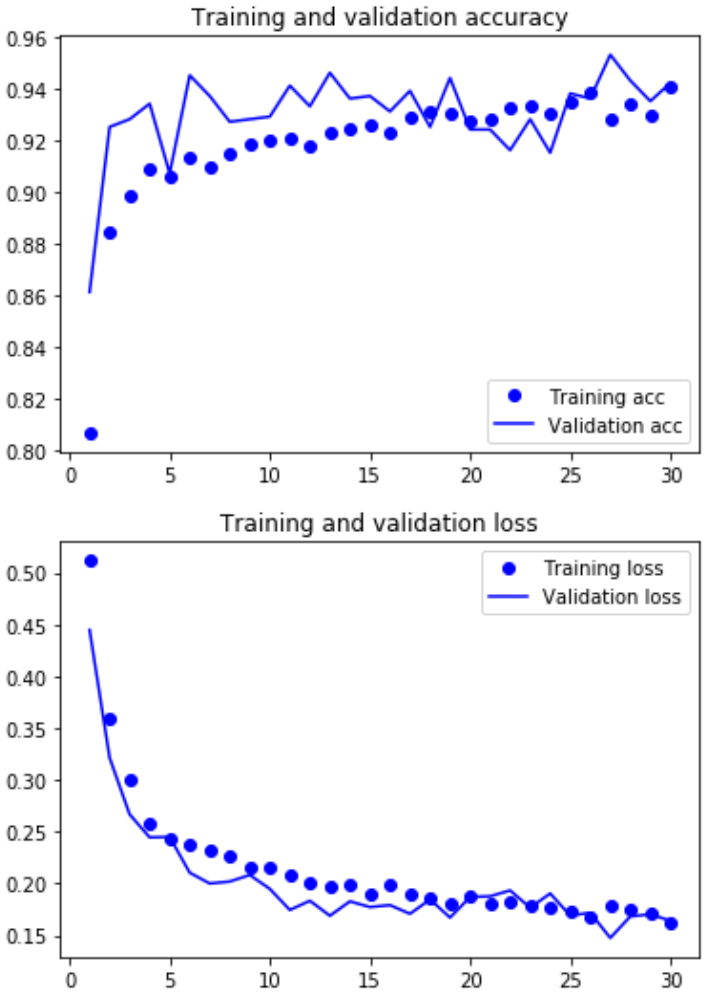

FIGURE 6. The accuracy and loss curves of the training and accuracy sets for 30 epochs for improved VGG model

The relationship between the number of FFT point and resolution: In liborsa, the temporal resolution is the ability to distinguish the immediate impact in the time domain. Frequency resolution shows the ability to distinguish adjacent single-frequency tones in the frequency domain. It appears that the smaller the L, the larger the time resolution; and the larger the N fft, the larger the frequency resolution. In fact, high resolution cannot be selected only according to $L \leq N$ fft. When the length of each frame is not equal to the number of FFT points, it needs to be filled with zeros. But the zero padding operation cannot increase the frequency resolution. When the original data length remains unchanged, no matter how to increase the number of FFT points, the waveform frequency resolution cannot be improved. Adding zeros in the time domain or frequency domain can only increase the interpolation density in another domain, not the resolution.

Over-fitting and under-fitting: The number of training samples is not enough to train a model that can be generalized to new data. Data augmentation is used to improve the data to prevent overfitting. This work uses the read image in keras to perform multiple random transformations to achieve data enhancement. The seismic electromagnetic data is recorded sequentially a day, it can be performed by shift, shear, and flip. The enhanced data comes from the original image, in order to further reduce over-fitting, it is necessary to add a dropout layer before the model densely connected to the classifier dense, and use

the regularization method to discard the random vector elements. The determination of seismic electromagnetic signals is a binary classification problem, and binary crossentropy function can be used as a loss function to determine the performance of the algorithm. Gradient descent to the value of the input image of the convolutional neural network can be applied to maximize the response of a certain filter, obtain the image with the largest response of the selected filter.

6. **Conclusion.** The traditional method of identifying seismic waveforms is mostly to process the waveform of the seismic signal directly, such as empirical mode decomposition, which performs Hilbert-Huang transform (HHT) on the decomposed signal and extracts the first three intrinsic mode function (IMF)) The linear prediction cepstral coefficients (LPCC) characteristic parameter of the component. Then use hidden Markov model (HMM) to establish the identification model of natural earthquake and artificial blasting [28]. The processing method is computationally complex and has low repeatability.

There is no direct evidence and theoretical support for the exact correlation between the occurrence of electromagnetic anomalies and earthquakes. Using improved short-time Fourier transform (STFT) and VGG16 architecture neural network model, the method described in this work has good classification performance for electromagnetic anomalies and various seismic electromagnetic images, which can be used to understand seismic electromagnetic phenomena.

Acknowledgment. This work is partially sponsored by Natural Science Foundation of Hubei province of China (Grant No.ZRMS2020000813), Science for Earthquake Resilience of CEA (Grant No.XH18030), Jiangxi Provincial Department of Science and Technology (No.20192BBEL50038), and the Scientific Research Fund of Institute of Seismology and Institute of Crustal Dynamics, China Earthquake Administration, (Grand No.IS201726156).

REFERENCES

[1] Y. Gao, D. Wang, J. Wen, and C. Yao, Electromagnetic responses to an earthquake source due to the motional induction effect in a 2D layered model, *Geophysical Journal International*, vol.219, no.1, pp.563–593, 2019.

[2] X. Wang, S. Yong, B. Xu, and Z. Bai, Research and implementation of multi-component seismic monitoring system AETA, *Acta entiarum Naturalium Universitatis Pekinensis*, vol. 54, pp.487-494, 2017.

[3] X. Cai, Y. Chen, and D. Han, Nonnegative tensor factorizations using an alternating direction method, *Frontiers of Mathematics in China*, vol.8, pp.3–18, 2013.

[4] A. Guettiche, P. Guéguen, and M. Mimoune, Seismic vulnerability assessment using association rule learning: application to the city of Constantine, Algeria, *Natural Hazards*, vol. 86, pp.1223–1245, 2017.

[5] L. Zhang, G. Zeng, and J. Wei, Adaptive Region-Segmentation Multi-Focus Image Fusion Based on Differential Evolution, *International Journal of Pattern Recognition and Artificial Intelligence*, vol.33, no.3, 1954010, 2019.

[6] K Wang, P Xu, CM Chen, S Kumari, M Shojafar, M Alazab, Neural Architecture Search for Robust Networks in 6G-enabled Massive IoT Domain, *IEEE Internet of Things Journal*, vol.8, no.7, pp.5332–5339, 2021.

[7] E. K. Wang, S. P. Xu, C. M. Chen, N. Kumar, Neural-Architecture-Search-Based Multiobjective Cognitive Automation System, *IEEE Systems Journal*, vol.15, no.2, pp.2918–2925, 2021.

[8] S. M. Potirakis, A. Schekotov, and T. Asano, Natural time analysis on the ultra-low frequency magnetic field variations prior to the 2016 Kumamoto (Japan) earthquakes, *Journal of Asian Earth Sciences*, vol.154, pp.419–427, 2018.

[9] J. Li and T. Ji, Principal component analysis and local correlation tracking as tools for revealing and analyzing seismo-electromagnetic signal of earthquake, *Seismology and Geology*, vol.39, pp.517–535, 2017.
[10] T. Xie, X. Du, J. Liu, Y. Y. Fan, Z. H. An, and J. Y. Chen, Wavelet power spectrum analysis of the electromagnetic signals of Wenchuan Ms8.0 and Haiti Mw7.0 earthquakes, *Acta Seismologica Sinica*, vol.35, pp.61–71, 2013.
[11] D. Zhang, H. Ren, and Q. Huang, Numerical simulation study of co-seismic electromagnetic signals in porous media, *Chinese Journal of Geophysics*, vol.56, pp.2739–2747, 2013.
[12] N. T. Lin, D. Zhang, and K. ZHANG, Predicting distribution of hydrocarbon reservoirs with seismic data based on learning of the small-sample convolution neural network, *Chinese Journal of Geophysics*, vol.61, pp.4110–4125, 2018.
[13] T. Ren, M. N. Lin, and H. F. Chen, Seismic event classification based on bagging ensemble learning algorithm, *Chinese Journal of Geophysics*, vol.62, pp.383–392, 2019.
[14] Y. Han, S. S. Li, and F. M. Chen, The seismic anomaly data mining model based on machine learning, *Computer Integrated Manufacturing Systems*, vol.31, pp.319–322, 2014.
[15] Z. F. Li, M. A. Meier, and E. Hauksson, Machine learning seismic wave discrimination: Application to earth quake early warning, *Geophysical Research Letters*, vol. 45, pp. 4773–4779, 2018.
[16] Z. Y. Cai and Z. X. Ge, Using artificial intelligence to pick P-wave first-arrival of the microseisms: taking the aftershock sequence of wenchuan earthquake as an example, *Acta Scientiarum Naturalium Universitatis Pekinensis*, vol.55, pp.451–460, 2019.
[17] Y. K. Chen, Automatic microseismic event picking via unsupervised machine learning, *Geophysical Journal International*, vol.212, pp.88–102, 2018.
[18] K. K. Tseng, J. Lin, C. M. Chen, M. M Hassan, A fast instance segmentation with one- stage multi-task deep neural network for autonomous driving, *Computers & Electrical Engineering*, vol.93, 107194, 2021.
[19] F. Q. Zhang, T. Y. Wu, Y. Wang, R. Xiong, G. Y. Ding, P. G. Mei, L. Y. Liu, Application of quantum genetic optimization of LVQ neural network in smart city traffic network prediction, *IEEE Access*, vol.8, pp.104555-104564, 2020.
[20] C. C. Liu, X. A. Wang, S. S. Yong, and B. X. Xu, Data storage and security system for AETA multi -component seismic monitoring system, *Computer Technology and Development*, vol.28, pp.7–12, 2018.
[21] X. Zhou, X. X. He, and C. W. Zheng, Radio signal recognition based on image deep learning, *Journal on Communication*, vol.40, pp.114–124, 2019.
[22] J. Fan, T. Liu, and L. Hu, Time-varying spectrum estimation of earthquake ground motion via modern time-frequency analysis, *Journal of Vibration & Shock*, vol.26, pp. 79–80, 2007.
[23] Y. L Yi and M. Nima, Tasnet: time-domain audio separation network for real-time, single-channel speech separation, *Proc. of the IEEE Int'l Conf. on Acoustics, Speech and Signal Processing (ICASSP)*, Seoul, South Korea, pp. 696–700, 2018.
[24] C. Szegedy, W. Liu, and Y. Jia, Going deeper with convolutions *Proc. of the IEEE Int'l Conf. on Computer Vision and Pattern Recognition (CVPR)*, Boston, CA, USA, pp.1–9, 2015.
[25] J. M. T. Wu, Z. Li, G. Srivastava, J. Frnda, V. G. Diaz and J. C. W. Lin, A CNN-based Stock Price Trend Prediction with Futures and Historical Price, *Proc. of 2020 International Conference on Pervasive Artificial Intelligence (ICPAI)*, Taipei, Taiwan, pp.134–139, 2020.
[26] J. M. T. Wu, Z. Li, N. Herencsar, B. Vo, and J. C. W. Lin, A graph-based CNN-LSTM stock price prediction algorithm with leading indicators, *Multimedia Systems*, 2021, https://doi.org/10.1007/s00530-021-0075.
[27] C. Szegedy, S. Ioffe, V. Vanhoucke, and A. Alemi, Inception-v4, Inception-ResNet and the Impact of Residual Connections on Learning. Available: arXiv:1602.07261, 2016.
[28] N. E. Huang, M. L. Wu, and W. D. Qu, Applications of Hibert - Huang transform to non-stationary financial time series analysis, *Applied Stochastic Models in Bussiness and Idustry*, vol.19, pp.245–268, 2003.